

# Dynamic Synaptic Modulation of LMG Qubits populations in a Bio-Inspired Quantum Brain

J. J. Torres<sup>1,\*</sup> and E. Romera<sup>2</sup>

<sup>1</sup> Departamento de Electromagnetismo y Física de la Materia  
and Instituto Carlos I de Física Teórica y Computacional,  
Universidad de Granada, Fuentenueva s/n, 18071 Granada, Spain

<sup>1</sup> Departamento de Física Atómica, Molecular y Nuclear  
and Instituto Carlos I de Física Teórica y Computacional,  
Universidad de Granada, Fuentenueva s/n, 18071 Granada, Spain and

\* Corresponding author: J.J. Torres, email: [jtorres@onsager.ugr.es](mailto:jtorres@onsager.ugr.es)

We present a biologically inspired quantum neural network that encodes neuronal populations as fully connected qubits governed by the Lipkin-Meshkov-Glick (LMG) quantum Hamiltonian and stabilized by a synaptic-efficacy feedback implementing activity-dependent homeostatic control. The framework links collective quantum many-body modes and attractor structure to population homeostasis and rhythmogenesis, outlining scalable computational primitives – stable set points, controllable oscillations, and size-dependent robustness – that position LMG-based architectures as promising blueprints for bio-inspired quantum brains on future quantum hardware.

## I. INTRODUCTION

The study of learning and information processing is a central theme in neuroscience, neural networks theory, and artificial intelligence, drawing the attention of the scientific community for decades. Recently, these topics have extended for quantum systems. For instance, advances in quantum computing motivated the creation of autonomous systems properly designed to try to find the quantum advantage in information processing, giving rise to emerging fields such as quantum machine learning and quantum artificial intelligence [4, 15]. Within this context, several proposals have described autonomous quantum devices capable of estimating states or unitaries [17, 28], implementing quantum reinforcement learning [5, 13, 14, 27, 30, 56], and constructing quantum neural networks (QNNs) [12, 53]. Also, variational quantum algorithms have been developed recently and used for such tasks [11].

Theoretical models have been proposed for both single quantum neurons [8, 22, 47], and network architectures, including quantum perceptrons [40, 55] and Hopfield networks [45] whose computational properties and storage capacity have been recently reported [51]. Research in this area aims

to determine whether such quantum analogues can surpass classical neural networks in pattern recognition and classification and memory storage capacity, while also incorporating biological inspiration [48]. Within this scenario, typically in most of the recent works concerning developing of quantum neural networks, binary neurons are replaced by qubits with simplified interactions. However, most of the classical and biologically inspired neural network models emphasize the crucial role of synapses [3] – nonlinear elements responsible for transmitting information through pairwise processes such as neurotransmitter release and recycling and high-order interactions involving astrocyte’s control of synaptic transmission [33]. Thus, experimental neuroscience has shown that synapses are dynamic, activity-dependent mechanisms whose transmission efficiency can either decrease (synaptic depression) or increase (facilitation) with presynaptic activity [54]. These mechanisms have major computational consequences [50], influencing memory capacity [31, 52], dynamic memory formation [39, 49], and stochastic resonances during weak-signal processing [32]. They can also lead to an imbalance between excitation and inhibition, causing a quick explosive increase of excitatory activity that originates intriguing brain waves [41] with different information content [34].

Building on these previous insights, recently has been proposed a quantum synapse framework incorporating synaptic plasticity, in which a quantum system with biologically inspired activity-dependent coupling between qubits was analyzed to study the effects of synaptic depression on qubit interactions and entanglement [48]. However, that model was limited to a small-scale system of only two qubits, which does not adequately represent the behavior of large quantum networks. Furthermore, the detailed treatment of qubit interactions in that study makes the approach less practical for extending to systems with many qubits, as the dimensionality of the state space increases rapidly with system size.

The Lipkin–Meshkov–Glick (LMG) Hamiltonian is a compact yet highly expressive framework for exploring quantum many-body phenomena. Originating in nuclear physics [24–26, 43], it provides a controlled setting for analyzing particle–particle and particle–hole correlations among neutrons and protons, as well as for benchmarking approximate many-body techniques. Its applicability extends well beyond that context, e.g. in condensed-matter physics it offers an effective description of Bose–Einstein condensates and Josephson-junction dynamics [23, 35, 36]. Also in optical physics, it has been used for the metrological quantification of spin-squeezed states and the engineering of multipartite entanglement, both in the presence of an external field and for the quadratic collective-spin Hamiltonian in the absence of a field [18, 20, 21, 42]. Taken together, the LMG model has become a standard tool for modeling collectively interacting two-level quantum systems. Within

this framework, the existence of first-, second-, and third-order quantum phase transitions (QPTs) has been demonstrated [10, 16]. More recently, it has been established that the associated quantum phase diagrams can be rigorously characterized in terms of phase-space delocalization measures, complemented by entanglement-entropy measures [6, 7, 9, 38, 44]. In what follows, we focus on the formulation of the LMG model that arises naturally in one-dimensional lattices of interacting spins – namely, an anisotropic  $XY$  (Ising-type) model in a transverse field with all-to-all couplings.

With this in mind, we here propose for the first time a quantum neural system biologically inspired including some level of short-term synaptic plasticity in the system and which is based in this LMG model. Such theoretical proposal includes two main features which should be considered while trying to build a *quantum brain*, namely, the system emergent properties represent the collective behavior of a system of  $N$  interacting quantum neurons or qubits, and it includes a sort of homeostatic plasticity self regulating the level of collective excitations in the system similar to short-term synaptic plasticity present in actual brains [1, 2, 29, 46, 57].

Interestingly, the dimensionality of this system remains computationally manageable, as its cost scales polynomially with system size. This property enables the study of collective behaviors in large quantum neural architectures, in contrast to microscopic quantum models where the Hilbert space dimension grows exponentially with the number of qubits. Moreover, our framework can be viewed as a minimal building block for constructing more complex quantum brain-like systems without a dramatic increase in computational complexity.

The system can be also implemented through a quantum circuit that can be executed in a quantum computer. It also provides a platform to explore novel emergent phenomena – such as quantum memory and learning processes – with potential applications in quantum machine learning.

## II. BIOLOGICALLY INSPIRED QUANTUM BRAIN MODEL

In this paper, we propose a model for collective oscillations within a *quantum brain* paradigm. Specifically, we describe this *quantum brain* as a set of  $N$  quantum neurons represented by qubits, such that an activated neuron corresponds to the excited state  $|1\rangle$  and an inactive neuron corresponds to the ground state  $|0\rangle$ . To model this *brain*, we employ the Lipkin-Meshkov-Glick (LMG) Hamiltonian and incorporate a synaptic biological mechanism akin to that introduced for the interaction of two neurons in [48].

By interpreting the quantum states of the LMG model as the quantum states of this brain, we obtain a clear analogy with actual brains, where one similarly defines collective oscillatory states

in both healthy (e.g., resting state; up/down cortical states during the wake–sleep transition; task-related collective states) and pathological (e.g., epileptic seizure states) conditions. In this way, it becomes possible to classify the quantum states of the model in a manner analogous to how neuroscientists classify empirical brain rhythms.

We now describe the quantum-brain model. To represent the states of this system we use the LMG Hamiltonian. The model consists of  $N$  mutually interacting two-level systems with infinite-range coupling, i.e., each particle can interact with any other. We begin with the intensive Hamiltonian

$$H' = \frac{\varepsilon}{N} \sum_{i=1}^N \sigma_i^z + \sum_{i < j} \frac{\gamma_x}{N(N-1)} \sigma_i^x \sigma_j^x + \sum_{i < j} \frac{\gamma_y}{N(N-1)} \sigma_i^y \sigma_j^y, \quad (1)$$

which models a lattice of  $N$  spin-1/2 particles with infinite-range (all-to-all)  $XY$  interactions, characterized by homogeneous couplings  $\gamma_x, \gamma_y$ . To connect this intensive representation with the collective formulation in terms of total-spin operators  $J_\alpha = \frac{1}{2} \sum_{i=1}^N \sigma_i^\alpha$ , we identify parameters via  $h = -2\varepsilon/N$ ,  $g = -(\gamma_x + \gamma_y)/(N-1)$ ,  $\gamma = (\gamma_x - \gamma_y)/(\gamma_x + \gamma_y)$ .

With these definitions, the Hamiltonian assumes the canonical collective form

$$H_{\text{LMG}} = -\frac{g}{N} \left[ (1 + \gamma) J_x^2 + (1 - \gamma) J_y^2 \right] - h J_z, \quad (2)$$

which is equivalent to (1) up to an inobservable additive constant (zero-point energy). Since  $[J^2, H_{\text{LMG}}] = 0$ , the dynamics decomposes into sectors of fixed total angular momentum  $j$ . In particular, the ground state resides in the maximally symmetric subspace  $j = N/2$ , a fact that markedly reduces spectral complexity. Here  $h$  is an external field and the parameter  $\gamma$  is an anisotropic parameter controlling the lack of rotational symmetry in the  $XY$  plane, i.e. the relative weight of pairing terms. In what follows and for simplicity, we shall work with the quadratic collective-spin Hamiltonian in the absence of an external field, i.e.,  $h = 0$ . The extension of the present study for cases with non-zero  $h$  can be related with the situation in which our quantum brain is receiving external stimuli from outside of the system as in classical neural networks, or from the senses in actual brains. The consideration of non-zero  $h$  can be interesting but it is beyond the scope of the present work and it will be considered in further studies.

To account for dynamical processes affecting qubits interactions similar to those reported in [48], we consider  $g(t) = g_0 r(t)$  where  $r(t)$  is a dimensionless, time-dependent coupling modulation, and  $g_0$  is a maximum coupling constant. Additionally, we assume that the time-dependent coupling modulation  $r(t)$  evolves according to a differential equation inspired by models of short-term synaptic depression, characterized by a recovery time  $\tau$  and a time-dependent release probability

$U(t)$  to account also for a synaptic facilitation mechanism:

$$\dot{r}(t) = f(r(t), \langle J_z \rangle, \tau_r, U(t)).$$

with

$$\dot{U}(t) = g(U(t), \langle J_z \rangle, \tau_f, \mathcal{U})$$

where  $\mathcal{U}$  is the release probability in absence of synaptic facilitation. The variable  $r(t)$  will represent then the hypothetical level of short-term synaptic plasticity in the *quantum brain*. The modulation  $r(t)$  is dynamically linked to the quantum evolution (via the von Neumann equation), producing a nonlinear feedback term in the dynamics of the quantum brain and to the evolution of the release probability  $U(t)$ :

$$\frac{d\rho(t)}{dt} = -\frac{i}{\hbar} [H(t), \rho(t)], \quad (3)$$

$$\frac{dr(t)}{dt} = \frac{1 - r(t)}{\tau_r} - U(t) r(t) \langle E \rangle_t, \quad (4)$$

$$\frac{dU(t)}{dt} = \frac{\mathcal{U} - U(t)}{\tau_f} + \mathcal{U}(1 - U(t)) \langle E \rangle_t, \quad (5)$$

where the expectation value  $\langle \cdot \rangle_t$  is taken with respect to  $\rho(t)$ .

Here,  $E$  is an operator that encodes a collective property of the quantum-brain model. The choice of  $E$  is quite general, enabling us to study how different observables shape the emergent dynamics. As a first step, and in line with the neuroscience analogy, we consider

$$E(t) = \frac{1}{2} + \frac{J_z(t)}{N}, \quad (6)$$

which quantifies the level of collective excitation in the quantum brain.

In the next section, we present the main results obtained with this quantum-brain model.

### III. RESULTS

#### A. Emerging Collective states in the quantum brain model

The first thing we observe when analyzing the system is the very rich dynamical behaviour depending on many dynamical aspects it includes as, for instance, the considered initial quantum state and the different values of system's relevant parameters. The system size also plays a main role

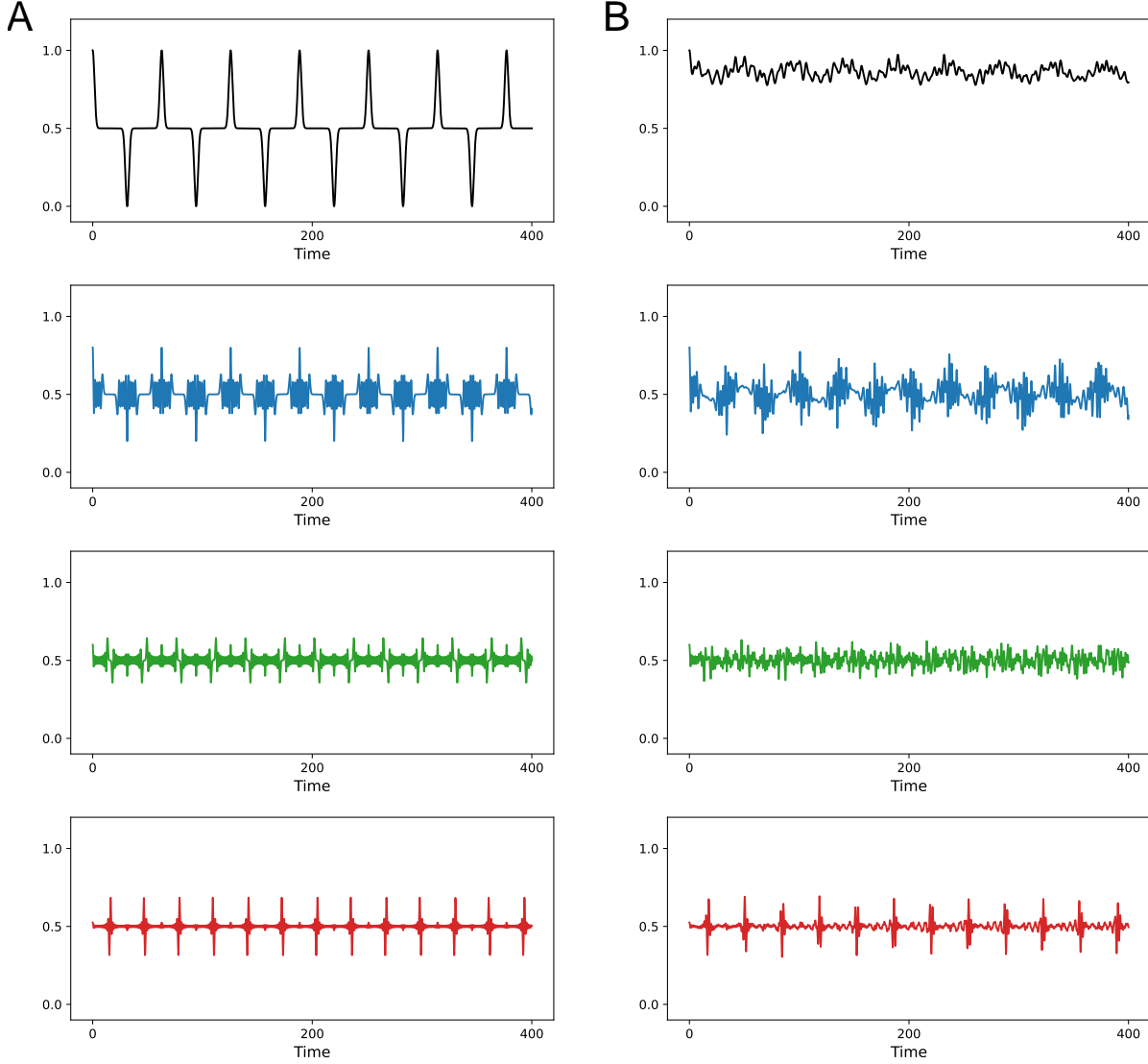


Figure 1: Particular dynamical behavior emerging in our quantum brain model, starting from different initial states with different perception of excited neuronal qubits corresponding from top to bottom to 100%, 80%, 60%, 53%. Panel (A) correspond to  $\gamma = 1$  and (B) to  $\gamma = 0.9$  respectively. Other parameters were  $g_0 = 2$  and  $\tau_r = 0$ .

since it increases the number of possible quantum states that can be reached during the quantum evolution of the system as we will see below.

As an initial look at the system's behaviour, in figure 1 we illustrate some typical oscillatory behaviour emerging in the system starting from different initial quantum states for some relevant parameters and for the case of  $N = 40$ . For comparison purposes we consider the cases  $\gamma = 1$  and  $\gamma = 0.9$ .

Next, we studied in more detail how the dynamical behavior of the system changes when system size and the initial state are varied. Thus, we characterize the dynamics of our *quantum brain* architecture under different initial conditions defined over the population state of the qubit neuronal population. The first observation in this neuronal-qubit system is that, when the initial condition corresponds to an exactly symmetric semi-activation (data not shown), the system becomes indefinitely trapped in the same quantum state, independently of the system size  $N$ . In neurodynamic terms, population activity remains strictly stationary over time (without fluctuations), such that no transitions or oscillations among microstates emerge.

Secondly, we consider an initial state of population semi-activation, in which approximately (but not exactly) half of the neuronal qubits are excited, as illustrated in figure 2. The temporal evolution of this fraction is denoted by  $\langle E(t) \rangle$ . We have explored different network sizes but we illustrate here the cases  $N = 10$  (left panel) and  $N = 80$  (right panel) for  $\gamma = 1$  and  $g_0 = 0.05$ . In the figure we display the averaged fraction (or count) of excited neuronal qubits  $\langle E(t) \rangle$  as a function of time, alongside the time course of synaptic efficacy  $r(t)$ . The temporal windows are adjusted to optimize the readability of dynamical regimes ranging from 0 to 4000 units for  $N = 10$ , and from 0 to 10000 for  $N = 80$ .

The results of our study reveal a strong anticorrelation between  $r(t)$  and  $\langle E(t) \rangle$ , similar to what is observed in biological systems: when population activity (the number of excited qubits) reaches its maximum, it leads to a reduction in synaptic efficacy, which subsequently reaches a relative minimum. Conversely, when the level of excited qubits is at its minimum, the synaptic efficacy recovers and attains its maximum value.

On average, the system remains near the  $(N/2)$  operating point, consistent with population-level homeostasis. As  $N$  increases, the network exhibits enhanced neurodynamic stability: the variability of  $E(t)$ , i.e., the oscillation amplitude of the excited fraction, progressively diminishes, indicating more effective gain control and a more confined attractor landscape. Nevertheless, on longer timescales, transient excursions (spikes) in the excited fraction emerge; even so, synaptic efficacy acts as a negative feedback loop that promotes re-stabilization toward the initial population-activation set point.

Third, we consider a fully silent initial condition in which no neuronal qubit is excited (see figure 3). This scenario is analyzed with the same neuronal-qubit population size as in the preceding case and over identical temporal windows. Although the level of synaptic depression is not very high ( $\tau_r = 1$ ), the figure suggests that synaptic efficacy can function as a homeostatic feedback mechanism. Initially, relatively low values of  $r(t)$  facilitate the activation of excited units when

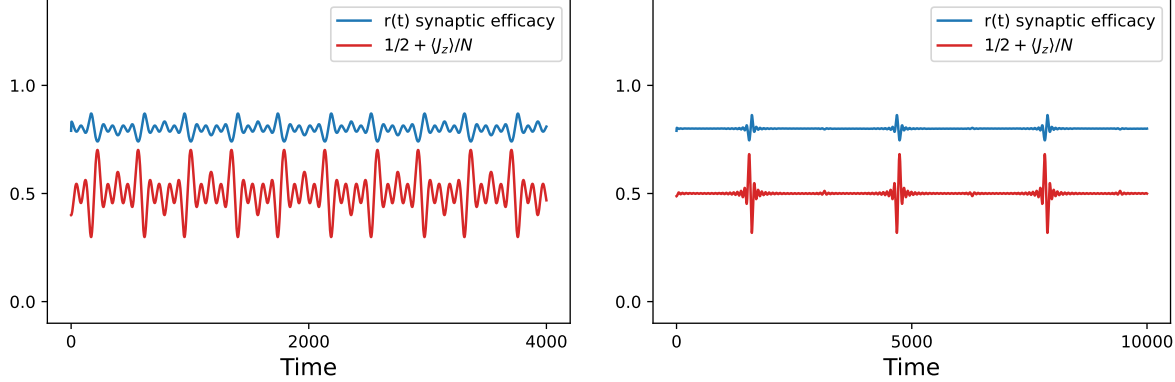


Figure 2: Time evolution of the number of excited neuronal qubits  $1/2 + \langle J_z \rangle / N$  and synaptic efficiency  $r(t)$  for (left)  $N = 10$ , and (right)  $N = 80$  neuronal qubits. Initial state: around half of the neuronal qubits are excited. Other parameters were  $\gamma = 1$ ,  $g_0 = 0.05$  and  $\tau_r = 1$ .

overall activity is low, leading to the growth of the red line toward its maximum. This, in turn, triggers a subsequent decrease in synaptic efficacy (the blue line declining toward its minimum). At this point,  $r(t)$  begins to limit the proliferation of excited units as activity peaks, causing a decline in activation (the red line decreasing after the maximum) and allowing  $r(t)$  to recover (the blue line rising after the minimum). This interplay generates a predominantly oscillatory global dynamic in the system.

Moreover, as network size increases, the dwell time within a metastable regime – where approximately half of the neuronal qubits remain excited – lengthens. Nevertheless, the dynamics exhibit periodic excursions toward extreme states – fully quiescent (0 % excited) or fully saturated (100% excited) – which are actively corrected by synaptic homeostasis as explained above, preventing fixation in these boundary attractors and restoring population balance.

Finally, it is noteworthy that, starting from an initial condition with no neuronal activity, the temporal evolution of the system spontaneously converges toward a population-level activity pattern consistent with the network normal operating regime.

Lastly, we consider a fully saturated initial state in which all neuronal qubits are excited. The corresponding behavior is illustrated in Fig. 4. Once again, synaptic efficacy operates as a homeostatic negative feedback loop: it compensates for the hypersaturated initial condition and steers the network toward a progressive reduction in the fraction of excited units. When the dynamics cross the minimal activity threshold (i.e., enter regions approaching population quiescence) the same

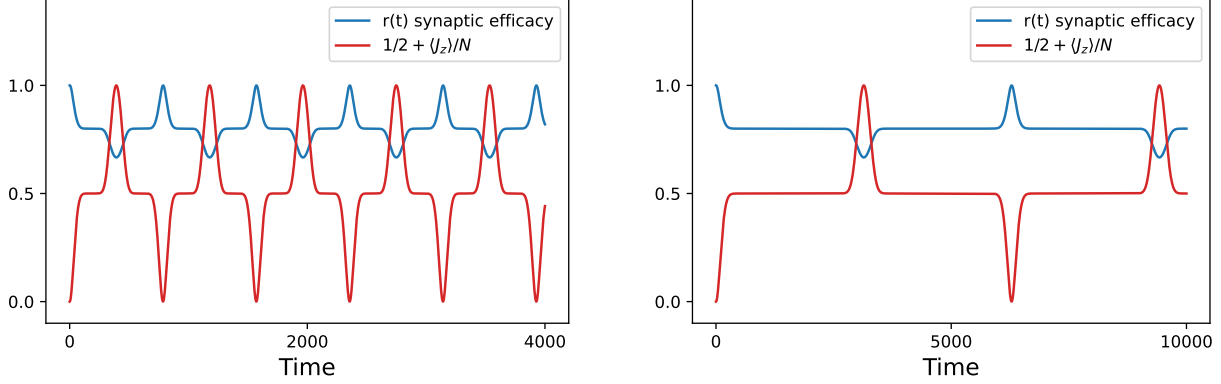


Figure 3: Time evolution of the number of excited neuronal qubits  $1/2 + \langle J_z \rangle/N$  and synaptic efficiency  $r(t)$  for (left)  $N = 10$ , and (right)  $N = 80$  neuronal qubits. Initial state: no neuronal qubit is excited. Other parameters were  $\gamma = 1$ ,  $g_0 = 0.05$  and  $\tau_r = 1$ .

synaptic efficacy effectively reverses its action and promotes the recruitment of activity, preventing fixation in the silent state.

Consistent with the preceding cases, increasing network size lengthens the intervals of residence around the population operating point near  $N/2$  (a metastable regime). Nevertheless, the temporal trajectory exhibits periodic excursions toward boundary attractors: episodes of overshoot with transient elevation to near-total activation, followed by undershoot with de-excitation that can reach complete silencing (0 excited qubits). These cycles of over- and under-correction are damped by synaptic homeostasis, which restores population balance and maintains the dynamics around the network functional set point.

In the figure 5 we represent the temporal evolution of the fidelity measured as  $|A(t)|^2$  with  $A(t)$  being the time autocorrelation function. The left panel corresponds to an initial state with all neuronal qubits excited (the behaviour of the system is analogous when one starts with a state with no excited qubits). On the other hand, the right panel shows the dynamics for an initial states with approximatively half of the qubits being excited.

In the first scenario, one identifies a temporal structure characterized by a well-defined periodicity, in which the initial state is reinstated at a fixed frequency after the system has traversed the entirety of its possible states. In the second scenario, the dynamics oscillate in the vicinity of the initial state, departing from it only moderately and exhibiting bounded fluctuations with an equally well-defined periodicity.

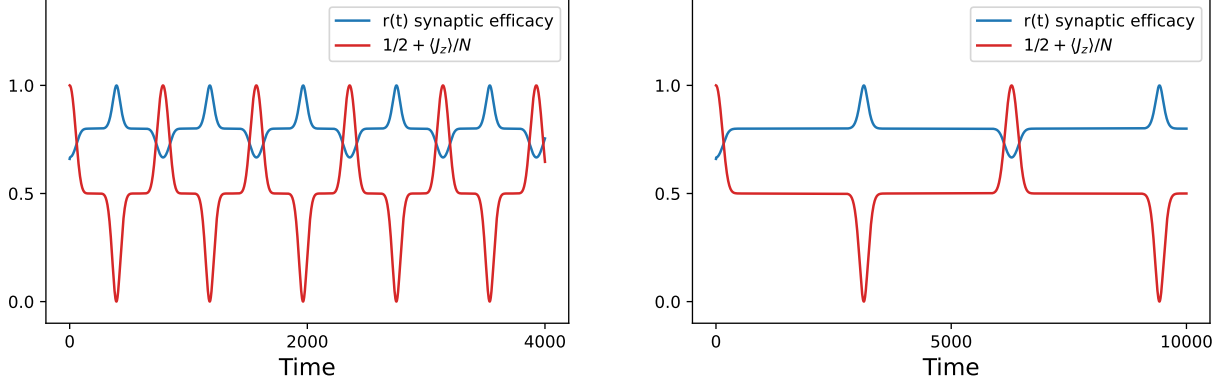


Figure 4: Time evolution of the number of excited neuronal qubits  $1/2 + \langle J_z \rangle / N$  and synaptic efficiency  $r(t)$  for (left)  $N = 10$ , and (right)  $N = 80$  neuronal qubits. Initial state: all neuronal qubits are excited. Other parameters were  $\gamma = 1$ ,  $g_0 = 0.05$  and  $\tau_r = 1$ .

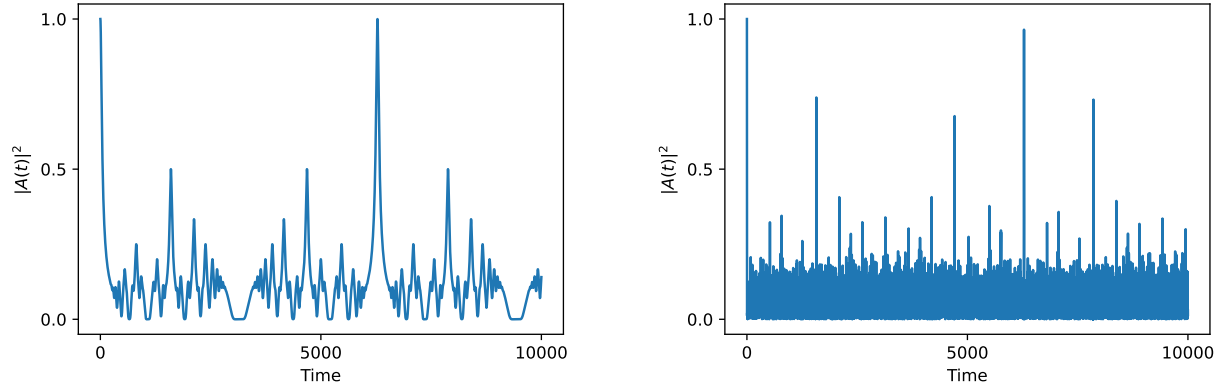


Figure 5: Time evolution of the fidelity neuronal qubits for an initial state with (left) no neuronal qubits excited or all the neuronal qubits excited, (right) around half of the neuronal qubits excited ( $N/2 - 1$ ), with parameters  $N = 80$ ,  $\gamma = 1$ , initial synaptic efficacy  $r_0 = 1$ ,  $U = 0.5$

To quantify the entanglement through the evolution of the system let's consider a bipartition  $L | (N-L)$  of the Hilbert space and take a block of  $L = \lfloor N/2 \rfloor$ . In the symmetric subspace the reduced matrix of this block is diagonal in the Dicke base with probabilities

$$p_k^{(L)} = \sum_{n=0}^N |c_n|^2 \frac{\binom{L}{k} \binom{N-L}{n-k}}{\binom{N}{n}}, \quad k = 0, \dots, L, \quad (7)$$

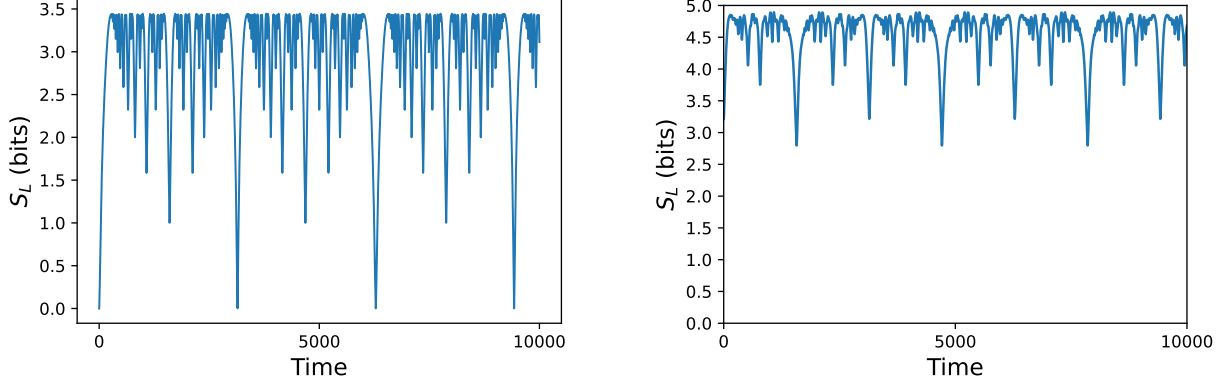


Figure 6: Von Neumann entropy  $S_L$  time evolution of the neuronal qubits for an initial state with (left) no neuronal qubits excited or all the neuronal qubits excited, (right) around half of the neuronal qubits excited ( $N/2 - 1$ ), with parameters  $N = 80$ ,  $\gamma = 1$ , initial synaptic efficacy  $r_0 = 1$ ,

$$U = 0.5$$

in such a way that the von Neumann entropy of the block is given by

$$S_L = - \sum_{k=0}^L p_k^{(L)} \log_2 p_k^{(L)}.$$

The figure 6 shows the time evolution of  $S_L$  for  $N = 80$ , using the same parameters as in the previous simulations. When the initial state has all qubits excited,  $S_L$  evolves from 0 (a pure, non-entangled state) to a maximum close to 3.46 and periodically returns to values close to zero. Whenever the system approaches its initial state, the bipartite entanglement between subblocks is transiently suppressed.

Conversely, when the initial state has approximately half of the qubits excited,  $S_L$  remains at relatively high values throughout the evolution: it starts around 3.3, increases to reach maximum values of about 4.8, and only exhibits periodic relative minima slightly below the initial value, never approaching zero. These relative minima coincide in time with the peaks of  $E(t)$ , indicating brief intervals in which the global state acquires a somewhat simpler structure and the bipartite entanglement between subblocks is partially reduced.

## B. The effect of synaptic plasticity on collective states

We have next studied the effect of the synaptic feedback in Eq. 4 on the features of the emergent collective dynamics of our *quantum brain* system. At the beginning we are going to consider only

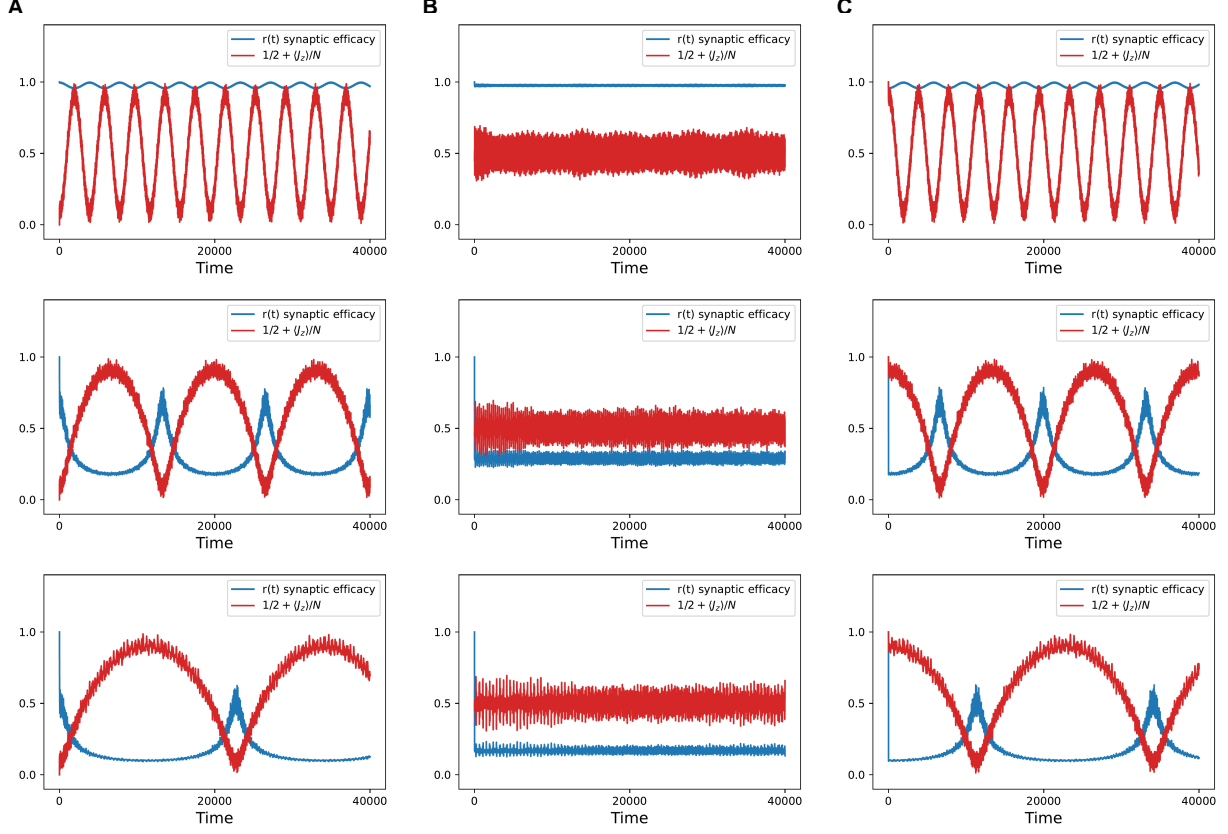


Figure 7: Effect of the synaptic plasticity feedback mechanisms on LMG collective dynamics for three different initial states corresponding to (A) no neuronal qubits excited, (B) around half of the neuronal qubits excited ( $N/2 - 1$ ) and (C) all the neuronal qubits excited. From top to bottom y each panel the parameter  $\tau$  controlling the synaptic plasticity feedback has been increased taking the values  $\tau_r = 0.1, 10, 20$ . Other parameters are  $N = 20$ ,  $g_0 = 0.5$ ,  $\gamma = 0.8$ ,

$$U(t) = \mathcal{U} = 0.5 \text{ and } r_0 = 1.$$

the effect of synaptic depression dynamics [39, 52, 54], but the model can be easily extended for more complex dynamics including synaptic facilitation [19, 31, 49]. The results are summarized in the figure 7. We consider here  $\gamma < 1$  to account for an asymmetry in the terms appearing in the LMG hamiltonian which helps to better visualize the effect of the synapse feedback on the emergent properties of the LMG system. We also compared the effect of quantum synaptic plasticity when one starts in the same three initial states considered in the previous analysis and that are illustrated, respectively, on panels (A) for an initial unexcited state, panel (B) for a intermediate half population of qubits excited state, and (C) for an initial all qubits excited state. When the

level of synaptic feedback is low (top panels in all cases corresponding to  $\tau = 0.1$ ), i.e.  $r(t) \approx 1$ , one observes at short time scales that the activity of the system is correlated with the corresponding initial state presenting very high frequency oscillations corresponding to collective many-body Rabi oscillation. However at relatively large time scale (low frequency) the system additionally shows symmetric up/down collective oscillations similar to Rabi oscillations of a single qubit dynamics. Such oscillations have a typical frequency of  $2.5 \times 10^{-4}$  oscillations per unit time for the set of parameters considered. The oscillatory behavior is symmetric between up and down temporal phases (that is the lower and larger energy states are populated identically during the oscillations) and depends on the parameters of the LMG models such as  $\gamma, g_0$  and  $N$  (in this case we are considering  $N = 20$ ). In fact it is a property of the LMG model. When synaptic feedback start to be important which is produced by increasing the value of  $\tau_r$  – middle and bottom panels – there is a clear coupling between the intrinsic dynamics of the LMG system and the synaptic plasticity feedback. The main consequence of such interplay is that the shape of the oscillations dramatically changes in different ways. First, the frequency of the oscillations strongly decreases with  $\tau_r$  and secondly a strong asymmetry in the population of the low energy and high energy levels of the LMG occurs, in such a way that the synaptic feedback favors the population of the high-energy levels when one starts initially at the low energy and at the high energy levels. Interestingly, when one starts at the half populated energy level the system does not show clear low frequency collective oscillations independently of the level of synaptic feedback present in the system – see panel B – and synaptic feedback only affect the high-frequency collective many-body Rabi oscillation. The asymmetry in the population of the LMG model induced by the synaptic feedback in the other cases is more strong when  $\tau_r$  is larger.

To obtain a clearer picture of how synaptic depression affects the behavior of the collective states in the present quantum-brain model, we computed the evolution of the linear entropy  $S_L$  for different values of  $\tau_r$ . Figure 8 compares the temporal evolution of the linear entropy  $S_L(t)$ , and the corresponding power spectra for three increasing levels of synaptic depression. In the absence of depression (top row),  $S_L(t)$  displays fast and highly regular oscillations, alternating between low-entropy episodes associated with the extrema of the collective spin dynamics and high-entropy intervals in the transition regions among these low-entropy states. When depression is introduced (middle and bottom rows), a pronounced asymmetry emerges between high- and low-entropy levels, indicative of an imbalance in the transition periods between non-excited and excited states, and vice versa, which in turn results in different time scales for the intervals of high entanglement. This conclusion is corroborated by analyzing in parallel the power spectrum

of  $S_L(t)$ , which, in the absence of depression, exhibits a dominant, narrow, high-frequency peak associated with a well-defined frequency, a clear periodicity and, ultimately, a single characteristic time scale for the high-entropy intervals. By contrast, as depression increases, this peak shifts to lower frequencies and additional harmonics emerge. Furthermore, the main maximum broadens, revealing a progressive blurring of the dominant entropy oscillation and a larger dispersion of the characteristic frequencies. This behavior is consistent with the emergence of longer entanglement or transition periods (in particular during the passage from non-excited to excited states) and with a less sinusoidal signal, compatible with a persistent population imbalance between the extreme collective states. Taken together, these results indicate that synaptic depression generally slows down and blurs the near-periodic dynamics of the system and, on average, favors more highly entangled states.

#### IV. THE ROLE OF SYNAPTIC FACILITATION

We have also explored the role that synaptic facilitation has on the emergence of collective spin states in our quantum brain model. The main findings are summarized in Figure 9. In this analysis we taken three different values of system size  $N = 2$  (panel A), 10 (panel B), and 20 (panel C). Moreover, we used a small value of the parameter  $\mathcal{U} = 0.02$  compared with the previous case of synaptic depression in order to see the effect of the synaptic facilitation whose main consequence at the biological level is to increase the release probability  $U(t)$  as given by Eq. 5 during a time scale of  $\tau_f$ . We also consider a different value of  $g_0$  for any value of the system size to have the same temporal scale for population state oscillations and to have a better comparison analysis. Then we increase the facilitation time constant  $\tau_f$  for any  $N$  depicted in panels A, B, and C from top to bottom. Note that  $\tau_f \approx 0$  means that only synaptic depression is present in the system, which in this case since we have an small value of  $\mathcal{U} = 0.02$  will correspond to a relatively large level of synaptic depression feedback with  $r(t)$  below 0.5 – see blue line in the top panel of A, B and C. Also in this situation facilitation of the release probability never occur so one has  $U(t) \approx \mathcal{U}$  (see solid green line in all top panels). When one increases  $\tau_f$  (time series from top to bottom in panels A, B and C) we are increasing the time period at which  $U(t)$  increases (facilitates). This makes the release probability to increases until it reaches a value  $U(t) \approx 1$  corresponding to  $r(t) \approx 0$  during any period of large excitation in the system as depicted in the bottom panels. Note that a large value of  $U(t)$  also implies an strong depression effect – see Eq. 4. The main consequence is that increasing  $\tau_f$  helps to increase the imbalance between non-excited and excited collective

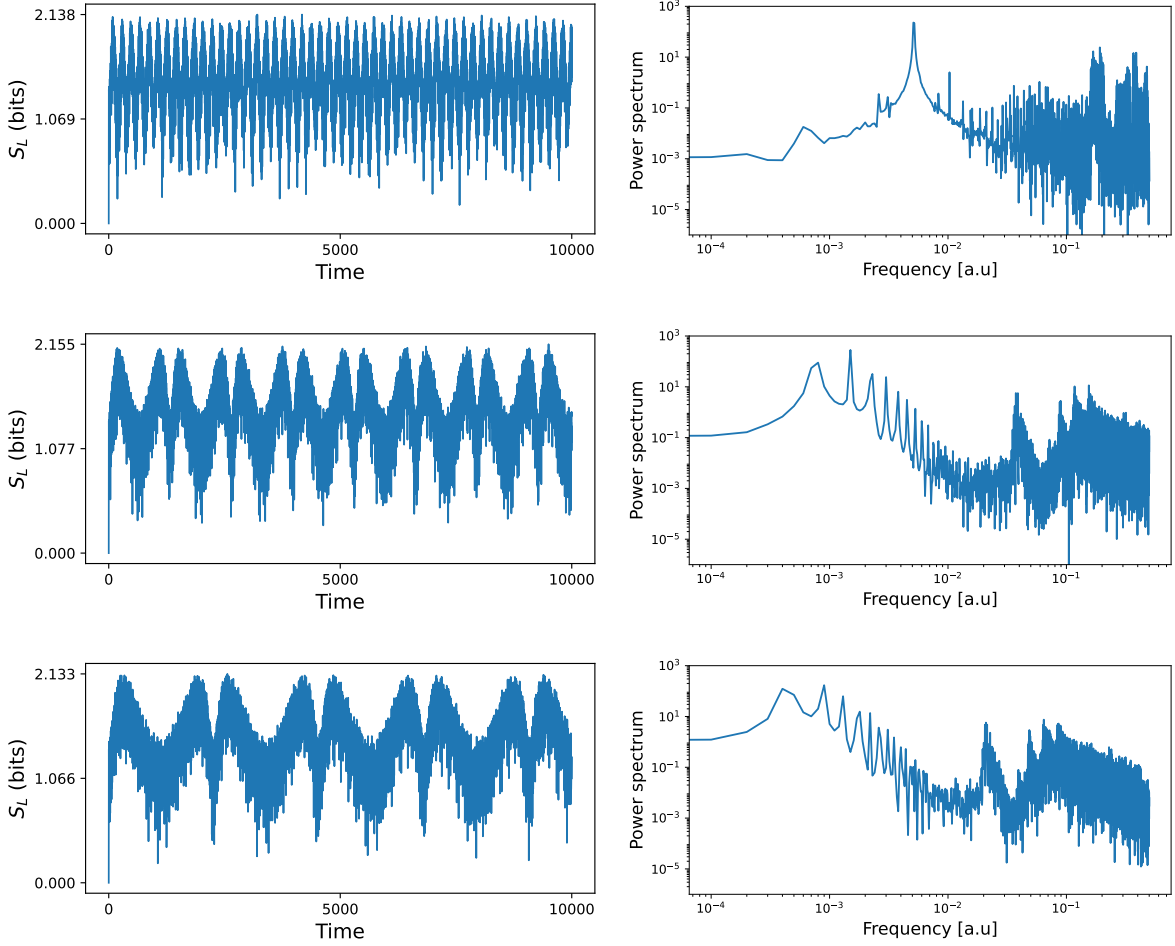


Figure 8: Temporal evolution of the linear entropy  $S_L(t)$  (left panel), stationary probability distribution of  $S_L$  (central panel), and power spectrum of  $S_L(t)$  (right panel) for three increasing levels of synaptic depression (top to bottom). In the absence of depression,  $S_L$  periodically and quickly alternates between low- and high-entropy regimes, but being most of the time between these two states, resulting in an effectively unimodal distribution at a relatively large intermediate value of the entropy. The corresponding spectrum shows a narrow peak at high frequency. As depression increases, the distribution shifts toward higher entropies emerging a second high-entropy peak. The corresponding spectrum shows a peak that moves to lower frequencies with additional secondary harmonics, as depression increasing indicating longer entanglement periods and increased dwell times in highly entangled states.

states. Moreover facilitation also induces a systematic imbalance in the transition periods between non-excited and excited collective states and vice versa (see collective oscillations in red color in the middle panels in A, B, C). Our study also illustrated that, independently of the system size,

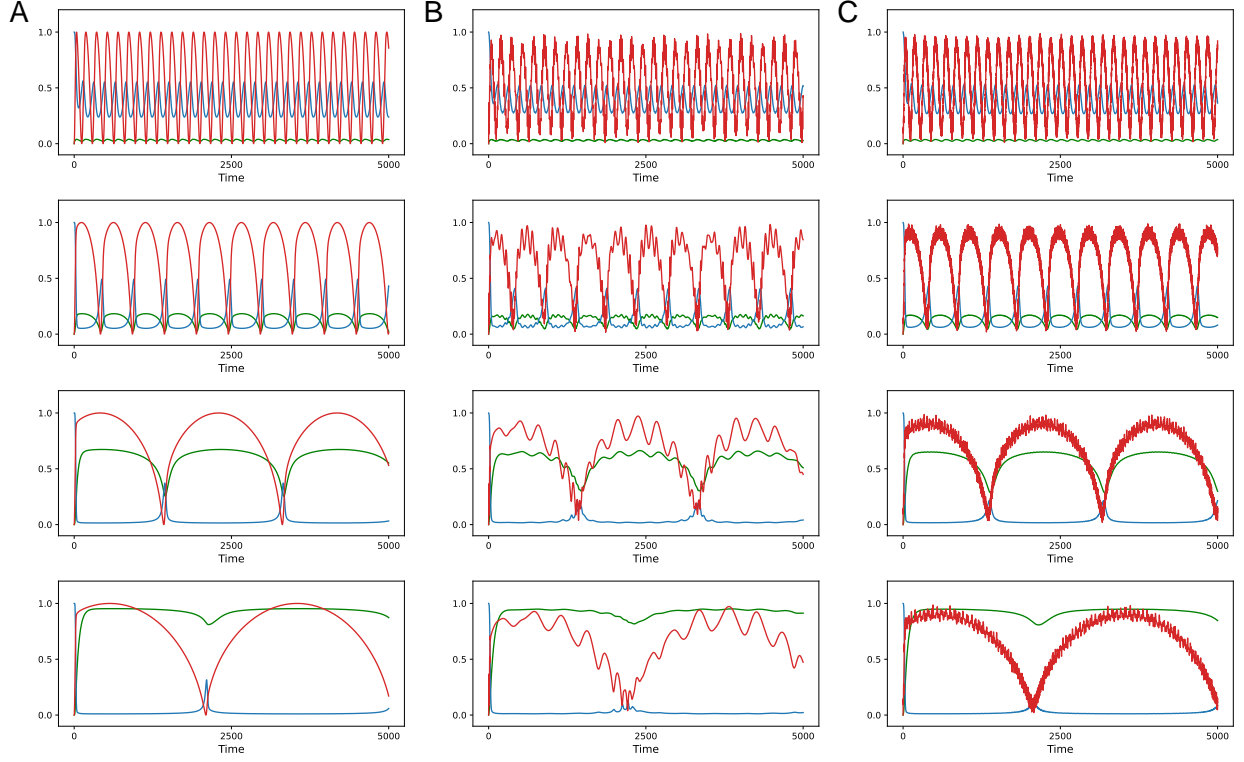


Figure 9: The effect of synaptic facilitation on the behaviour of the LMG brain model. The figure shows the cases of system sizes of  $N = 2$  (A)  $N = 10$  (B) and  $N = 20$  (C) for  $\tau_f = 1, 10, 100, 1000$  from top to bottom respectively. For each  $N$  we consider a particular choice for  $g_0$  in order to recover the same temporal scale in all cases, son one has  $g_0 = 0.125$  (A),  $g_0 = 1.43$  (B) and  $g_0 = 30$  (C). In each panel it is plotted the level of excitation in the system measured in terms of  $1/2 + \langle J_z \rangle / N$  (red line), the level of synaptic feedback measured with  $r(t)$  (blue line) and the release probability  $U(t)$  (green line). One can observe that independently of the system size, the effect of synaptic feedback and facilitation is the same after properly rescaling the coupling  $g_0$ .

Other parameter were  $\gamma = 0.8$   $\tau_r = 100$  and  $\mathcal{U} = 0.02$ .

the effect of facilitation is more or less the same after properly chosen other parameters as  $g_0$  in this case. This is not surprisingly since in the LMG hamiltonian we have a global  $N$  rescaling  $g_0$ .

## V. CONCLUSIONS

In this work we have presented a theoretical framework to develop a *quantum brain* paradigm. Such framework is based in the well known LMG model for the study of qubit population states together with a synaptic homeostatic feedback motivated from neuroscience. In this way, we can

build and study a quantum system that show qubits collective states whose dynamics is controlled by the level of synaptic feedback present in the system. This approach aims to reproduce, at the quantum level, collective activity states similar to those observed in actual brains.

Our study shows that the quantum brain model introduced here exhibits different homeostatic population dynamics, in such a way that if it starts quiescent or saturated, activity quickly converges to a regime with  $\approx N/2$  excited qubits that acts as a metastable attractor. Larger networks stabilise this operating point, reducing fluctuations of the excited fraction  $E(t)$  and increasing the time spent near it. Similarly to what occurs in actual neural systems, synaptic efficacy in our quantum system provides a negative-feedback loop that suppresses excessive activity and boosts low activity.

From a quantum perspective, the dynamics depend strongly on the initial state. For ordered configurations (all qubits excited or none), the fidelity attains maximum values equal to one, at which the global state periodically recovers its initial form. The bipartite von Neumann entropy  $S_L$  rises from zero to a maximum and returns to values close to zero when the fidelity reaches unity, indicating a transient suppression of bipartite entanglement. In contrast, for semi-activated initial states (with  $\approx N/2$  excited qubits),  $S_L$  remains high and its minima never reach zero. These minima coincide with the peaks of  $E(t)$ , signaling brief episodes in which the system passes close to the initial state, accompanied only by a partial reduction of bipartite entanglement. Taken together, the model combines homeostatic regulation with quantum entanglement features that are strongly determined by the initial preparation.

Synaptic feedback in the LMG-based “quantum brain” model reconfigures collective behavior in a way that is very similar to synaptic plasticity in biological circuits. Under weak feedback (small  $\tau_r$ ,  $r(t) \approx 1$ ), the system displays high-frequency many-body Rabi oscillations constrained by the initial state and slower, symmetric oscillations between low- and high-energy sectors reflecting the bare LMG dynamics. As synaptic feedback strengthens (large  $\tau_r$ ), plasticity and intrinsic dynamics become tightly coupled, lowering oscillation frequencies and introducing a systematic imbalance in energy-level occupation, with a growing bias toward high-energy states. The semi-activated initial condition acts as a special operating regime: it does not generate low-frequency collective oscillations for any  $\tau_r$ , and feedback only modulates the high-frequency Rabi cycles. Thus, quantum synaptic plasticity, without extra assumptions, plays a role analogous to biological synaptic regulation by tuning time scales and collective patterns and reorganizing, in a state-dependent way, the effective distribution of activity across energy levels via the parameter  $\tau_r$ .

We also observed that synaptic feedback strongly affect collective states entanglement in such a way that the periods of maximum entanglement corresponding to the transitions from the non-

excited to totally excited states enlarges. Also it introduces complexity in the system which is depicted by the emergence of non-periodicities in the time series of the lineal entropy.

Our study also shows that synaptic facilitation strongly influences the emergence and time structure of collective states dynamics in the quantum brain model. When facilitation is weak, the dynamics are dominated by synaptic depression, leading to more time symmetric and balanced transitions between activity states. As facilitation becomes stronger, the system exhibits prolonged periods of heightened release probability, which amplify depressive effects and create a stronger separation between excited and non-excited collective states. This also introduces a noticeable asymmetry in the transitions between these states. Overall, synaptic facilitation enhances the contrast in collective dynamics and also amplifies a systematic imbalance in collective state transitions, and these effects remain consistent across different system sizes when the model is appropriately rescaled.

The observed imbalance in the levels of the LMG model induced by the synaptic feedback could have interesting applications as for example the use of the LMG with this synaptic feedback for the design of quantum working memories similar to those already studied in neuroscience [37]. Variants of the present study could also include coupling of LMG systems with different synaptic feedback levels, each one favoring a particular level of quantum qubit populations.

Summing up, the present work represents an initial step toward constructing quantum formulations of biologically inspired neural systems. By doing so, we aim to uncover the potential computational consequences that may arise at the quantum level, particularly those linked to mechanisms that could provide a quantum advantage within biological contexts. This framework opens the door to exploring how quantum effects might enrich or transform the functional principles traditionally associated with neural computation. Additionally, the proposed model could be readily implemented in emerging quantum architectures, opening the door to the development of functional quantum brain prototypes in the near future.

## VI. ACKNOWLEDGMENTS

This work has been supported by Grant No. PID2023-149174NB-I00 financed by the Spanish Ministry and Agencia Estatal de Investigación MICIU/AEI/10.13039/501100011033 and ERDF funds (European Union). E.R. acknowledges support from PAIDI group FQM-420 of the University of Granada.

## VII. AUTHOR CONTRIBUTIONS

J.J.T and E.R. equally contributed to the conception, design, and research of the methods presented in this article. All authors equally contributed to the writing of the manuscript.

## VIII. COMPETING INTERESTS

The authors declare no competing interests.

---

[1] L. F. Abbott and W. G. Regehr. Synaptic computation. *Nature*, 431(7010):796–803, 2004.

[2] L. F. Abbott, J. A. Varela, K. Sen, and S. B. Nelson. Synaptic depression and cortical gain control. *Science*, 275(5297):221–224, 1997.

[3] Daniel J. Amit. *Modeling Brain Function*. Cambridge University Press, Cambridge, 2012.

[4] Jacob Biamonte, Peter Wittek, Nicola Pancotti, Patrick Rebentrost, Nathan Wiebe, and Seth Lloyd. Quantum machine learning. *Nature*, 549(7671):195–202, Sep 2017.

[5] Hans J. Briegel and Gemma De las Cuevas. Projective simulation for artificial intelligence. *Scientific Reports*, 2:400, 2012.

[6] M. Calixto, R. Romera, and R. del Real. Parity-symmetry-adapted coherent states and entanglement in quantum phase transitions of vibron models. *Journal of Physics A: Mathematical and Theoretical*, 45:365301, 2012.

[7] Manuel Calixto, Octavio Castaños, and Elvira Romera. Entanglement and quantum phase diagrams of symmetric multi-qubit systems. *Journal of Statistical Mechanics: Theory and Experiment*, 2017(10):103103, 2017.

[8] Yudong Cao, Gian Giacomo Guerreschi, and Alán Aspuru-Guzik. Quantum neuron: An elementary building block for machine learning on quantum computers. *arXiv preprint arXiv:1711.11240*, 2017.

[9] O. Castaños, M. Calixto, F. Pérez-Bernal, and E. Romera. Identifying the order of a quantum phase transition by means of wehrl entropy in phase space. *Physical Review E*, 92:052106, 2015.

[10] O. Castaños, R. López-Peña, J. Hirsch, and E. López-Moreno. Classical and quantum phase transitions in the lipkin–meshkov–glick model. *Physical Review B*, 74:104118, 2006.

[11] M. Cerezo, Andrew Arrasmith, Ryan Babbush, Simon C. Benjamin, Suguru Endo, Keisuke Fujii, Jarrod R. McClean, Kosuke Mitarai, Xiao Yuan, Lukasz Cincio, and Patrick J. Coles. Variational quantum algorithms. *Nature Reviews Physics*, 3(9):625–644, 2021.

[12] Simantini Chakraborty, Tamal Das, Saurav Sutradhar, Mrinmoy Das, and Suman Deb. An analytical review of quantum neural network models and relevant research. In *2020 5th International Conference on Communication and Electronics Systems (ICCES)*, pages 1395–1400, 2020.

- [13] Samuel Yen-Chi Chen, Chao-Han Huck Yang, Jun Qi, Pin-Yu Chen, Xiaoli Ma, and Hsi-Sheng Goan. Variational quantum circuits for deep reinforcement learning. *IEEE Access*, 8:141007–141024, 2020.
- [14] Daoyi Dong, Chunlin Chen, Hanxiong Li, and Tzyh-Jong Tarn. Quantum reinforcement learning. *IEEE Transactions on Systems, Man, and Cybernetics, Part B (Cybernetics)*, 38(5):1207–1220, 2008.
- [15] Vedran Dunjko and Hans J. Briegel. Machine learning and artificial intelligence in the quantum domain: a review of recent progress. *Reports on Progress in Physics*, 81:074001, 2018.
- [16] S. Dusuel and J. Vidal. Finite-size scaling exponents of the lipkin-meshkov-glick model. *Physical Review Letters*, 93:237204, 2004.
- [17] Dietmar G. Fischer, Stefan H. Kienle, and Matthias Freyberger. Quantum-state estimation by self-learning measurements. *Phys. Rev. A*, 61:032306, Feb 2000.
- [18] Zhiyao Hu, Qixian Li, Xuanchen Zhang, Long-Gang Huang, He-bin Zhang, and Yong-Chun Liu. Spin squeezing with arbitrary quadratic collective-spin interactions. *Phys. Rev. A*, 108(2):023722, August 2023.
- [19] Skyler L. Jackman and Wade G. Regehr. The mechanisms and functions of synaptic facilitation. *Neuron*, 94(3):447–464, 2017.
- [20] P. Jurcevic, B. P. Lanyon, P. Hauke, C. Hempel, P. Zoller, R. Blatt, and C. F. Roos. Quasiparticle engineering and entanglement propagation in a quantum many-body system. *Nature*, 511:202, 2014.
- [21] Masahiro Kitagawa and Masahito Ueda. Squeezed spin states. *Physical Review A*, 47:5138, 1993.
- [22] Lars Bojer Kristensen, Matthias Degroote, Peter Wittek, Alán Aspuru-Guzik, and Nikolaj Thomas Zinner. An artificial spiking quantum neuron. *npj Quantum Information*, 7:59, 2021.
- [23] A. J. Leggett. Bose–einstein condensation in the alkali gases: Some fundamental concepts. *Reviews of Modern Physics*, 73:307–356, 2001.
- [24] H. J. Lipkin, N. Meshkov, and A. J. Glick. Validity of many-body approximation methods for a solvable model: I. exact solutions and perturbation theory. *Nuclear Physics*, 62:188, 1965.
- [25] H. J. Lipkin, N. Meshkov, and A. J. Glick. Validity of many-body approximation methods for a solvable model: II. linearization procedures. *Nuclear Physics*, 62:199, 1965.
- [26] H. J. Lipkin, N. Meshkov, and A. J. Glick. Validity of many-body approximation methods for a solvable model: III. diagram summations. *Nuclear Physics*, 62:211, 1965.
- [27] Owen Lockwood and Mei Si. Reinforcement learning with quantum variational circuit. In *Proceedings of the AAAI Conference on Artificial Intelligence and Interactive Digital Entertainment*, volume 16, pages 94–100, 2020.
- [28] Daniel Manzano, Marcin Pawłowski, and Časlav Brukner. The speed of quantum and classical learning for performing the  $k$ th root of not. *New Journal of Physics*, 11:113018, 11 2009.
- [29] Henry Markram, Joachim Lübke, Michael Frotscher, and Bert Sakmann. Redistribution of synaptic efficacy between neocortical pyramidal neurons. *Nature*, 382(6594):807–810, 1996.
- [30] Joshua Mautner, Adi Makmal, Daniel Manzano, Markus Tiersch, and Hans J. Briegel. Projective simulation for classical learning agents: A comprehensive investigation. *New Generation Computing*,

33(1):60–79, 2015.

[31] Jorge F. Mejías and Joaquín J. Torres. Maximum memory capacity on neural networks with short-term synaptic depression and facilitation. *Neural Computation*, 21:851–871, 2009.

[32] Jorge F. Mejías and Joaquín J. Torres. Emergence of resonances in neural systems: the interplay between adaptive threshold and short-term synaptic plasticity. *PLoS ONE*, 6:e17255, 2011.

[33] Gustavo Menesse, Ana P. Millán, and Joaquín J. Torres. Astrocyte-mediated higher-order control of synaptic plasticity. *arXiv preprint arXiv:2507.07693 [q-bio.NC]*, 2025.

[34] Gustavo Menesse and Joaquín J. Torres. Information dynamics of in silico EEG brain waves: Insights into oscillations and functions. *PLoS Computational Biology*, 20(9):e1012369, 2024.

[35] A. Micheli, D. Jaksch, J. I. Cirac, and P. Zoller. Many-particle entanglement in two-component bose-einstein condensates. *Physical Review A*, 67:013607, 2003.

[36] G. J. Milburn, J. Corney, E. M. Wright, and D. F. Walls. Quantum dynamics of an atomic bose-einstein condensate in a double-well potential. *Physical Review A*, 55:4318–4324, 1997.

[37] Gianluigi Mongillo, Omri Barak, and Misha Tsodyks. Synaptic theory of working memory. *Science*, 319(5869):1543–1546, 2008.

[38] A. Nagy and E. Romera. Fisher information, rényi entropy power and quantum phase transition in the dicke model. *Physica A*, 391:3650, 2012.

[39] Lovorka Pantic, Joaquín J. Torres, Hilbert J. Kappen, and Stan C. A. M. Gielen. Associative memory with dynamic synapses. *Neural Computation*, 14:2903–2923, 2002.

[40] Miroslav Pechal, Finn Roy, Samuel A. Wilkinson, Gian Salis, Max Werninghaus, Michael J. Hartmann, and Stefan Filipp. Direct implementation of a perceptron in superconducting circuit quantum hardware. *arXiv preprint arXiv:2111.12669*, 2021.

[41] Jorge Pretel, Joaquín J. Torres, and Joaquín Marro. EEGs disclose significant brain activity correlated with synaptic fickleness. *Biology*, 10(7):647, 2021.

[42] P. Richerme, Z.-X. Gong, A. Lee, C. Senko, J. Smith, M. Foss-Feig, S. Michalakis, A. V. Gorshkov, and C. Monroe. Non-local propagation of correlations in quantum systems with long-range interactions. *Nature*, 511:198, 2014.

[43] Peter Ring and Peter Schuck. *The Nuclear Many-Body Problem*. Springer, New York, 1980.

[44] E. Romera, M. Calixto, and A. Nagy. Entropic uncertainty and the quantum phase transition in the dicke model. *Europhysics Letters*, 97:20011, 2012.

[45] Pietro Rotondo, Matteo Marcuzzi, Juan P. Garrahan, Igor Lesanovsky, and Markus Müller. Open quantum generalisation of hopfield neural networks. *Journal of Physics A: Mathematical and Theoretical*, 51(11):115301, 2018.

[46] Charles F. Stevens. Facilitation and depression at single central synapses. *Neuron*, 14(4):795–802, 1995.

[47] Francesco Tacchino, Chiara Macchiavello, Dario Gerace, and Daniele Bajoni. An artificial neuron implemented on an actual quantum processor. *npj Quantum Information*, 5:26, 2019.

- [48] J J Torres and D Manzano. A model of interacting quantum neurons with a dynamic synapse. *New Journal of Physics*, 24:073007, 7 2022.
- [49] Joaquín J. Torres, Jesus M. Cortes, Joaquín Marro, and Hilbert J. Kappen. Competition between synaptic depression and facilitation in attractor neural networks. *Neural Computation*, 19:2739–2755, 2007.
- [50] Joaquín J. Torres and Hilbert J. Kappen. Emerging phenomena in neural networks with dynamic synapses and their computational implications. *Frontiers in Computational Neuroscience*, 7:30, 2013.
- [51] Joaquín J. Torres and Daniel Manzano. Dissipative quantum hopfield network: a numerical analysis. *New Journal of Physics*, 26:103018, 10 2024.
- [52] Joaquín J. Torres, Lovorca Pantic, and Hilbert J. Kappen. Storage capacity of attractor neural networks with depressing synapses. *Physical Review E*, 66:061910, 2002.
- [53] E. Torrontegui and J. J. García-Ripoll. Unitary quantum perceptron as efficient universal approximator. *EPL (Europhysics Letters)*, 125:30004, 3 2019.
- [54] Misha Tsodyks, Klaus Pawelzik, and Henry Markram. Neural networks with dynamic synapses. *Neural Computation*, 10(4):821–835, 1998.
- [55] Nathan Wiebe, Ashish Kapoor, and Krysta M. Svore. Quantum perceptron models. In *Proceedings of the 30th Conference on Neural Information Processing Systems (NeurIPS 2016)*, 2016.
- [56] Tong Xiao, Jie Fan, and Guihua Zeng. Parameter estimation in quantum sensing based on deep reinforcement learning. *npj Quantum Information*, 8(1):2, 2022.
- [57] Robert S. Zucker and Wade G. Regehr. Short-term synaptic plasticity. *Annual Review of Physiology*, 64(1):355–405, 2002.